

Microvascular Function Regulates Intestinal Crypt Response to Radiation

Jerzy G. Maj, François Paris,¹ Adriana Haimovitz-Friedman, Ennapadam Venkatraman, Richard Kolesnick,² and Zvi Fuks^{2,3}

Laboratory of Signal Transduction and the Departments of Radiation Oncology and Biostatistics, Memorial Sloan-Kettering Cancer Center, New York, New York 10021

Abstract

Recent evidence suggests that microvascular endothelial apoptosis represents the primary lesion in radiation damage to the gastrointestinal (GI) tract. Rescue of endothelium by depletion of *acid sphingomyelinase* or i.v. treatment with basic fibroblast growth factor (FGF) prevented the lethal GI syndrome in C₅₇Bl/6 mice. Here we show that basic FGF increased crypt survival after irradiation by 2–3 fold, with a dose modification factor at D₁₀ of 1.15 ($P < 0.01$). Basic FGF inhibited initial crypt damage, assessed by crypt shrinkage at 18–24 h, but did not significantly affect the regeneration of surviving crypts at 3.5 days after irradiation. These data suggest that microvascular function regulates expression of radiation-induced crypt stem cell clonogen damage in the evolution of radiation injury to the GI mucosa.

Introduction

Despite intensive research over the past two decades, the mechanism by which radiation induces damage to the GI⁴ mucosa remains only partially known. There is a general consensus that dysfunction of the intestinal clonogenic compartment, located near the bottom of the crypt of Lieberkühn, is a critical element in this process (1–3). The clonogenic compartment consists of a pool of pluripotent GI stem cells and early undifferentiated progenitors that possess a multilineage clonogenic potential (2–5). The GI mucosa is a rapid turnover system, driven by the mitotic activity of its clonogens. This activity generates, at a constant rate, lineages of transit cells that differentiate into end-stage columnar epithelium as they multiply and migrate toward the villus. At the villus, differentiated epithelial cells continue to migrate toward its tip, at which they shed into the intestinal lumen via the villus extrusion zone. A delicate balance between the rates of crypt cell proliferation, cell migration, and extrusion through the tip of the villus maintains the architectural integrity of the intestinal mucosa. The lifetime of an epithelial GI cell from generation at the clonogenic compartment to extrusion is 3–5 days. This rapid cycling time constitutes the basis for the high sensitivity of the GI mucosa to radiation and to other stresses that affect the integrity of its clonogenic compartment (2, 3).

A body of work by Potten *et al.* (2, 3) has described the sequence of events after exposure to doses ≥ 8 Gy, required to induce GI damage. Serial histological examinations revealed little apoptotic activity in the crypt epithelium during the first 24 h after irradiation, except for a p53-dependent apoptotic response at positions 4–5 that does not appear associated with the pathogenesis of the GI syndrome.

However, [³H]thymidine and bromodeoxyuridine labeling studies revealed a late S-phase mitotic arrest of crypt clonogens (6), coupled with continued epithelial cell migration along the crypt-villus axis and extrusion from the villus tip (7). The outcome of this combined response is progressive crypt shrinkage during the first 24–36 h after irradiation (2). Villus shrinkage may eventually commence if crypt depletion is fairly advanced or complete. Release from mitotic arrest occurs at ~ 36 h and is associated with a rapid increase in the proliferative activity of the clonogens that have not migrated and remained at their original crypt location (8). It is assumed, although not conclusively proven, that during this phase, proliferating clonogens may undergo mitotic or postmitotic cell death. At doses < 15 Gy, surviving progenitors, albeit even a single surviving clonogen per crypt, lead to crypt recovery, identified by 3.5 days after irradiation as typical hyperplastic regenerative crypts that exceed the size of control crypts by more than 2-fold (9–11). Large regenerating crypts split or bud to generate new crypts, until the intestinal mucosa regains a normal architecture at about 2 weeks after irradiation (2, 9). At doses ≥ 15 Gy, extensive depletion of crypt-villus units leads to mucosal denudation and animal death from the GI syndrome (2). Although this model defines a critical role for clonogenic cells in the pathogenesis of GI damage, the regulation of this response remains unknown, because there are no specific markers that identify this population.

We have recently addressed this issue demonstrating that radiation-induced apoptosis of the crypt microvascular endothelium constitutes an essential element in the pathogenesis of the radiation-induced GI syndrome (12). Our data indicated a close correlation between the severity of crypt dysfunction and the intensity of microvascular endothelial apoptosis. The GI syndrome was prevented when endothelial cell apoptosis was inhibited genetically by depletion of the *acid sphingomyelinase* (*ASMase*) gene or pharmacologically by i.v. injection of bFGF (12), known to inhibit the proapoptotic function of *ASMase* in endothelial cells (13). Furthermore, *in situ* hybridization studies showed that endothelial cells, but not other crypt cells, expressed bFGF receptor mRNA transcripts either before or after irradiation (12), providing compelling evidence that the endothelium of the crypt microvasculature is the target for the radioprotective effect of bFGF. These studies did not, however, define whether microvascular damage links to the induction of crypt shrinkage, to the capacity of crypts to undergo regeneration, or to another phase in the evolution of the GI syndrome. Here we show that endothelial rescue by bFGF improves crypt survival after irradiation. It results from the inhibition of radiation-induced crypt shrinkage and not from the enhancement of crypt regeneration. These studies provide evidence that microvascular endothelial apoptosis is ordered upstream of the mitotic dysfunction of the clonogenic compartment that occurs during the early phase of radiation-induced damage to the intestines.

Materials and Methods

Mice. C₅₇Bl/6 male mice, 8–12 weeks old, were purchased from The Jackson Laboratory (Bar Harbor, Maine). Mice were housed at the animal core facility of Memorial Sloan-Kettering Cancer Center. This facility is approved

Received 5/8/03; accepted 6/17/03.

The costs of publication of this article were defrayed in part by the payment of page charges. This article must therefore be hereby marked *advertisement* in accordance with 18 U.S.C. Section 1734 solely to indicate this fact.

¹ Present address: INSERM Unit 463, Institut de Biologie, 9 quai Moncoussu, 44093 Nantes Cedex 01, France.

² R. K. and Z. F. contributed equally to these studies.

³ To whom requests for reprints should be addressed, at the Department of Radiation Oncology, Memorial Sloan-Kettering Cancer Center, 1275 York Avenue, New York, NY 10021. Phone: (212) 639-5868; Fax: (212) 794-3188; E-mail: fuksz@mskcc.org.

⁴ The abbreviations used are: GI, gastrointestinal; bFGF, basic fibroblast growth factor; WBR, whole body radiation.

by the American Association for Accreditation of Laboratory Animal Care and is maintained in accordance with the regulations and standards of the United States Department of Agriculture and the Department of Health and Human Services, NIH.

Radiation, bFGF Treatment, and Tissue Preparation. WBR was delivered with a Shepherd Mark-I unit (Model 68, SN643) operating ^{137}Cs sources. The dose rate was 2.5 Gy/min. Human recombinant bFGF from SCIOS (Sunnyvale, CA) was solubilized in sterile PBS containing 0.2% gelatin and was delivered i.v. by retro-orbital injection of 800 ng at 10 min before irradiation and at 5, 60, and 120 min after irradiation. To obtain small intestinal samples, mice were sacrificed by hypercapnia asphyxiation, and 2.5-cm segments of proximal jejunum were obtained at 2 cm from the ligament of Trietz. Tissue samples were fixed by overnight incubation in 4% neutral buffered formaldehyde and embedded in paraffin blocks. Transverse tissue sections of the full jejunal circumference (5 μm thick) were obtained by microtomy from the paraffin blocks, adherence to polylysine-treated slides, and deparaffinizing by heating at 90°C for 10 min and at 60°C for 5 min, followed by two xylene washes for 5 min, and staining with H&E according to a standard protocol.

Crypt Size and Microcolony Assay. Crypts were identified histologically according to the criteria established by Withers and Elkind (9, 14, 15). Crypts were scored for width, height and area at 0–24 h and at 3.5 days after WBR using a calibrated Zeiss AxioHOME microscope. Thirty crypts were measured for each data point. Width was determined at the middle of the longitudinal crypt section. Height was measured from the bottom of the crypt to the crypt-villus junction. Area was calculated as width \times height in μm^2 . Data were reported as mean \pm SE. The microcolony survival assay was performed as described by Withers and Elkind (15). Briefly, surviving crypts were defined as containing 10 or more adjacent chromophilic non-Paneth cells, at least one Paneth cell, and a lumen. The circumference of a transverse cross-section of the intestine was used as a unit. The number of surviving crypts was counted in each circumference. Four circumferences were scored per mouse and 4–5 mice were used to generate each data point. Data were reported as mean \pm SE.

Data Analysis. Crypt survival curves were calculated by the least square regression analysis of all of the data points, using a modification of the FIT software program (16). The program fits the curves by iteratively weighted least squares to each set of dose-survival data, estimates the covariates of the survival curve parameters and the corresponding confidence regions, and plots the survival curve. It also derives curve parameters, such as the D_0 (the reciprocal of the slope on the exponential portion of the curve, representing the level of radiosensitivity) and the N number (measuring the size of the shoulder). Mean values of crypt areas were compared using the Student t test.

Results and Discussion

At baseline, the proximal jejunum of the $C_{57}\text{Bl}/6$ mouse colony used in the present studies contained 152 ± 3 crypts per circumference (mean \pm SE). The mean crypt diameter was $44 \pm 1.5 \mu\text{m}$ and height $85.6 \pm 2.2 \mu\text{m}$, yielding a sectioned axial crypt area of $3778 \pm 135 \mu\text{m}^2$. Fig. 1 shows the jejunal crypt survival curve for mice exposed to different doses of WBR. The D_0 (mean \pm SE) was 1.542 ± 0.71 Gy, similar to D_0 values published for other mouse strains (17–20). bFGF, given i.v. in repeated 800-ng doses at 10 min before WBR and at 5, 60, and 120 min after irradiation, shifted the curve to a higher-dose range, without producing a significant change in the D_0 (1.556 ± 0.21). The N numbers, however, differed significantly (224 ± 72 for control mice and 653 ± 67 for the bFGF-treated animals; $P < 0.05$), indicating that the difference between the two survival curves was significant. Consistent with this observation, the number of crypts surviving the exposure to 10–15 Gy was increased 2–3-fold by bFGF treatment. The dose required to produce an isoeffect of 10% crypt survival (D_{10}) was 11.81 ± 0.54 Gy for control and 13.58 ± 1.8 Gy for the bFGF-treated mice ($P < 0.01$), indicating a dose-modifying factor of 1.15 for the bFGF treatment protocol used in this study. These data confirm previous observations on the radioprotective effect of bFGF on intestinal crypt survival in other mouse strains (20, 21). The current experiments were, nonetheless, required as controls, because previous studies reported that the ability of

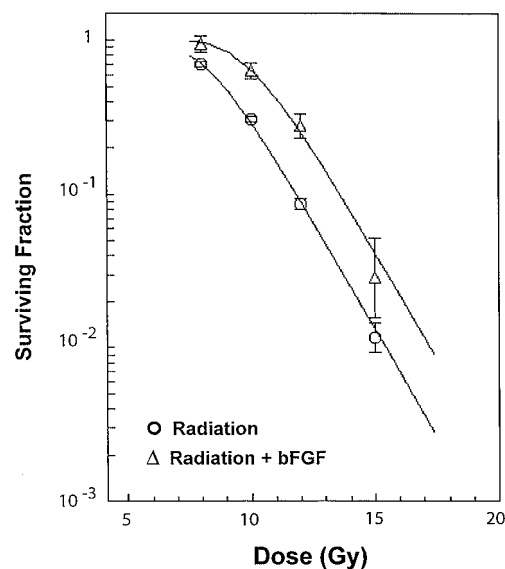


Fig. 1. Jejunal crypt survival curves for mice exposed to WBR. $C_{57}\text{Bl}/6$ mice were exposed to escalating doses of WBR. Human recombinant bFGF was injected i.v. at doses of 800 ng each at 10 min before irradiation and at 5, 60, and 120 min after irradiation. Samples of the proximal jejunum were obtained either before irradiation or at 3.5 days after irradiation, were fixed in formaldehyde, and were embedded in paraffin blocks. Transverse tissue sections of the full jejunal circumference (5 μm thick) were stained with H&E and scored for the number of regenerative crypts as described previously (15). Four circumferences were scored per mouse and five mice were used to generate each data point. Crypt survival curves were calculated by the FIT software program (16). Data are reported as mean \pm SE. Similar results were obtained in two experiments.

bFGF to modify the radiation effects in tissues was mouse-strain specific (22).

In Fig. 2A the effects of bFGF on radiation-induced crypt shrinkage are indicated within the first 24 h after WBR. In control mice receiving 10 Gy WBR, the crypt area decreased from $3778 \pm 135 \mu\text{m}^2$ in unirradiated controls to $3156 \pm 102 \mu\text{m}^2$ at 18 h ($P < 0.01$) and to $2437 \pm 86 \mu\text{m}^2$ at 24 h ($P < 0.01$). bFGF, given i.v. significantly protected against crypt shrinkage at all time points between 12 and 24 h after WBR ($P < 0.01$ versus irradiated alone), although mice receiving 10 Gy plus bFGF still manifested modest although statistically significant crypt shrinkage compared with unirradiated controls at 24 h (mean crypt area $3430 \pm 87 \mu\text{m}^2$; $P = 0.035$). Fig. 2B shows that the intensity of crypt shrinkage at 18 h after WBR was radiation dose dependent ($P < 0.01$ at all dose levels versus unirradiated controls). i.v. bFGF protected against crypt shrinkage at each radiation dose level ($P < 0.01$). In this regard, the level of crypt shrinkage at 15 Gy plus bFGF was similar to that observed at 10 Gy without bFGF. This finding is consistent with our previous studies demonstrating that neither treatment schedule resulted in death from the GI syndrome in $C_{57}\text{Bl}/6$ mice, whereas mice treated with 15 Gy alone succumbed to GI death (12).

Fig. 3 shows the effects of bFGF on regenerating crypts at 3.5 days after WBR. There was a 1.8–2.3-fold increase in irradiated crypt size ($P < 0.001$ at each dose level as compared with unirradiated controls). In contrast to the protective effect of bFGF against crypt shrinkage, there was no significant effect of bFGF on the size of regenerating crypts at any dose level (Fig. 3), even at 8 Gy, a dose that did not yield significant crypt shrinkage in bFGF-treated mice (Fig. 2B). Similarly, there was no effect of bFGF on the size of regenerating crypts at 4.5 days after WBR (not shown).

The present studies demonstrate that the radioprotective effect of bFGF targets the induction of initial crypt damage, rather than the subsequent regenerative phase. The protection afforded by bFGF resulted in an increase in the number of surviving crypts (Fig. 1), thus

improving the likelihood of restitution of the intestinal mucosa. Although the dose-modifying factor for the bFGF treatment protocol tested here was only 1.15, it was nonetheless sufficient to reduce crypt damage after 15 Gy WBR to the level observed in mice treated with ~13 Gy without bFGF. Our previous studies have identified 15 Gy WBR as a dose leading to death from the GI syndrome in C₅₇Bl/6 mice, whereas after 13 Gy, animals died from marrow aplasia with a fully recovered intestinal mucosa (12). The lack of an effect of bFGF on the proliferation of the crypt epithelium during the regenerative phase (Fig. 3) is consistent with our observation that crypt clonogens do not express receptors for bFGF either before or after exposure to radiation (12). The mechanism that activates crypt regeneration after irradiation is apparently independent of initial crypt damage, because large regenerative crypts were detected in bFGF-treated mice irradiated to 8 or 10 Gy (Fig 3), despite near complete protection from crypt shrinkage in these mice (Fig. 2A). Consistent with this notion, Houchen *et al.* (21) failed to disclose evidence of interaction of bFGF with regenerating crypt epithelial cells, despite immunohistochemical evidence for abundant bFGF in the lamina propria induced by the

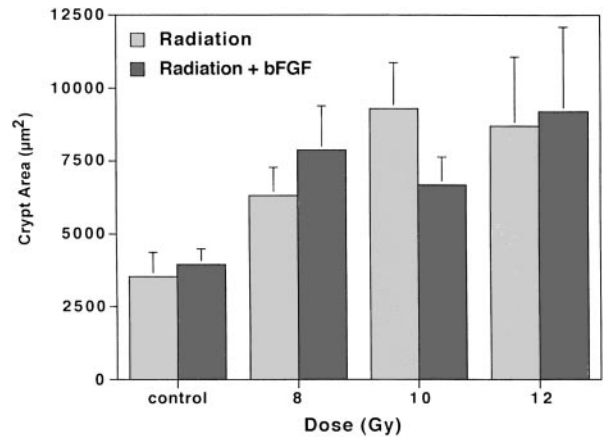


Fig. 3. Effect of bFGF on regenerative crypt size after WBR. C₅₇Bl/6 mice were treated, and tissue samples were obtained and processed as described in Fig. 2, except that crypts were scored either before irradiation or at 3.5 days after irradiation. Data are reported as mean ± SD. Similar results were obtained in two experiments.

Downloaded from <http://aacrjournals.org/cancerres/article-pdf/63/15/4338/2505620/oh1503004338.pdf> by guest on 22 June 2024

irradiation within hours after exposure to 13 Gy. In fact, this bFGF was in contact with blood vessels, perhaps providing a paracrine stimulation to the damaged or regenerating microvasculature.

Because the microvascular endothelium is the only crypt structure that expresses bFGF receptors and is directly rescued by bFGF from radiation-induced cell death (12), the present studies specifically order endothelial apoptosis upstream of crypt shrinkage in the intestinal radiation response. The prevention of crypt shrinkage by bFGF-mediated rescue of the microvascular endothelium suggests that microcirculatory function may regulate the crypt clonogen response to radiation. This hypothesis is consistent with our recent studies demonstrating that microvascular function regulates tumor cell survival at therapeutic dose levels of radiation (23). This paradigm diverges from the present consensus that clonogen dysfunction is an autonomous response to a direct interaction with radiation. It is conceivable that radiation does, in fact, directly induce lesions in crypt clonogens irrespective of endothelial cell damage, but that the expression of these lesions or their conversion into stimuli that induce mitotic arrest is conditionally dependent on a microvascular damage-mediated component. If such a linkage exists, it might be associated with leakage of a circulating factor, a bystander effect secondary to endothelial damage, or a response to transient local ischemia resulting from the apoptotic damage to the microvascular endothelium. In this regard, it should be noted that reduction of tissue oxygen induces in tumor cells the expression of a series of hypoxia-responsive genes (24). Additional studies are required to delineate this linkage.

The present studies define the mechanism mediating lethality in the GI syndrome. The pharmacological model system applied in the present studies allows ordering of the earliest events in crypt injury, supporting microvascular damage as causative in the loss/dysfunction of crypt stem cell clonogens. The studies also provide proof-in-principal that development of small molecules, such as bFGF, may serve to improve the toxic:therapeutic ratio during abdominal radiation therapy. Understanding the mechanism by which microvascular damage regulates normal and tumor tissue responses to radiation may have important clinical implications.

REFERENCES

- Hendry, J. H., Roberts, S. A., and Potten, C. S. The clonogen content of murine intestinal crypts: dependence on radiation dose used in its determination. *Radiat. Res.*, 132: 115-119, 1992.
- Potten, C. S. A comprehensive study of the radiobiological response of the murine (BDF1) small intestine. *Int. J. Radiat. Biol.*, 58: 925-973, 1990.

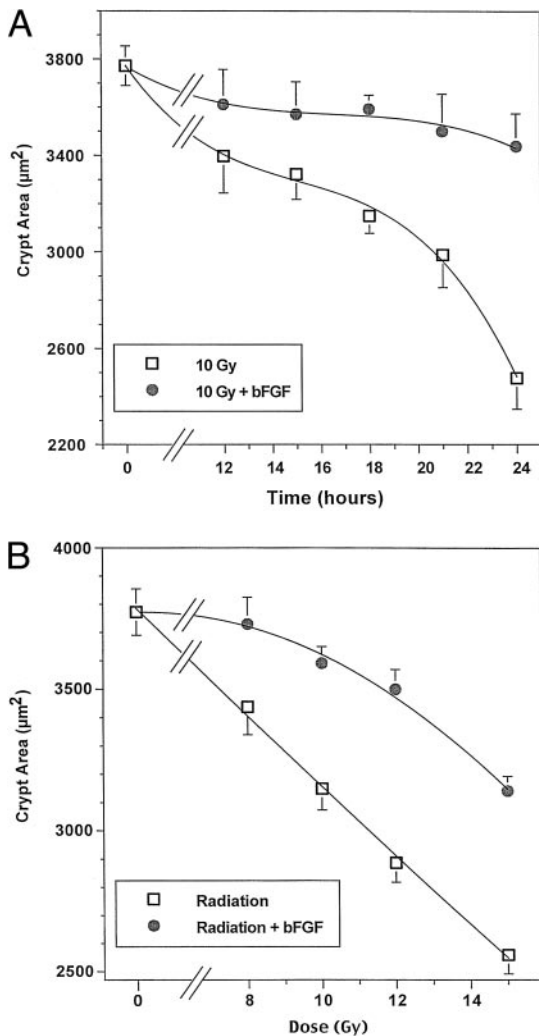


Fig. 2. Effect of bFGF on jejunal crypt shrinkage after WBR. C₅₇Bl/6 mice were exposed to escalating doses of WBR and human recombinant bFGF was delivered as described in Fig. 1. Samples of the proximal jejunum were obtained either before irradiation or at 12-24 h after irradiation and were stained with H&E as described in Fig. 1. Crypts were scored for width and height, and crypt area was calculated as width × height in µm². Ten to 20 crypts were scored for each data point. Data are reported as mean ± SE. A, effect of bFGF on crypt size at different time points after exposure to 10 Gy WBR. B, dose-response curves of crypt size in mice exposed to escalating doses of WBR with or without bFGF. Similar results were obtained in three experiments.

3. Potten, C. S., Booth, C., and Pritchard, D. M. The intestinal epithelial stem cell: the mucosal governor. *Int. J. Exp. Pathol.*, *78*: 219–243, 1997.
4. Gordon, J. I., and Hermiston, M. L. Differentiation and self-renewal in the mouse gastrointestinal epithelium. *Curr. Opin. Cell Biol.*, *6*: 795–803, 1994.
5. Marshman, E., Booth, C., and Potten, C. S. The intestinal epithelial stem cell. *Bioessays*, *24*: 91–98, 2002.
6. Chwalinski, S., Potten, C. S., and Evans, G. Double labelling with bromodeoxyuridine and [3H]-thymidine of proliferative cells in small intestinal epithelium in steady state and after irradiation. *Cell Tissue Kinet.*, *21*: 317–329, 1988.
7. Kaur, P., and Potten, C. S. Cell migration velocities in the crypts of the small intestine after cytotoxic insult are not dependent on mitotic activity. *Cell Tissue Kinet.*, *19*: 601–610, 1986.
8. Potten, C. S., Taylor, Y., and Hendry, J. H. The doubling time of regenerating clonogenic cells in the crypts of the irradiated mouse small intestine. *Int. J. Radiat. Biol.*, *54*: 1041–1051, 1988.
9. Withers, H. R. Regeneration of intestinal mucosa after irradiation. *Cancer (Phila.)*, *28*: 75–81, 1971.
10. Potten, C. S., and Hendry, J. H. Differential regeneration of intestinal proliferative cells and cryptogenic cells after irradiation. *Int. J. Radiat. Biol. Relat. Stud. Phys. Chem. Med.*, *27*: 413–424, 1975.
11. Potten, C. S., Rezvani, M., Hendry, J. H., Moore, J. V., and Major, D. The correction of intestinal microcolony counts for variation in size. *Int. J. Radiat. Biol. Relat. Stud. Phys. Chem. Med.*, *40*: 321–326, 1981.
12. Paris, F., Fuks, Z., Kang, A., Capodici, P., Juan, G., Ehleiter, D., Haimovitz-Friedman, A., Cordon-Cardo, C., and Kolesnick, R. Endothelial apoptosis as the primary lesion initiating intestinal radiation damage in mice. *Science (Wash. DC)*, *293*: 293–297, 2001.
13. Haimovitz-Friedman, A., Kan, C. C., Ehleiter, D., Persaud, R. S., McLoughlin, M., Fuks, Z., and Kolesnick, R. N. Ionizing radiation acts on cellular membranes to generate ceramide and initiate apoptosis. *J. Exp. Med.*, *180*: 525–535, 1994.
14. Withers, H. R., and Elkind, M. M. Dose-survival characteristics of epithelial cells of mouse intestinal mucosa. *Radiology*, *91*: 998–1000, 1968.
15. Withers, H. R., and Elkind, M. M. Microcolony survival assay for cells of mouse intestinal mucosa exposed to radiation. *Int. J. Radiat. Biol. Relat. Stud. Phys. Chem. Med.*, *17*: 261–267, 1970.
16. Albright, N. Computer programs for the analysis of cellular survival data. *Radiat. Res.*, *112*: 331–340, 1987.
17. Cai, W. B., Roberts, S. A., Bowley, E., Hendry, J. H., and Potten, C. S. Differential survival of murine small and large intestinal crypts following ionizing radiation. *Int. J. Radiat. Biol.*, *71*: 145–155, 1997.
18. Martin, K., Potten, C. S., Roberts, S. A., and Kirkwood, T. B. Altered stem cell regeneration in irradiated intestinal crypts of senescent mice. *J. Cell Sci.*, *111*: 2297–2303, 1998.
19. Khan, W. B., Shui, C., Ning, S., and Knox, S. J. Enhancement of murine intestinal stem cell survival after irradiation by keratinocyte growth factor. *Radiat. Res.*, *148*: 248–253, 1997.
20. Okunieff, P., Mester, M., Wang, J., Maddox, T., Gong, X., Tang, D., Coffee, M., and Ding, I. *In vivo* radioprotective effects of angiogenic growth factors on the small bowel of C3H mice. *Radiat. Res.*, *150*: 204–211, 1998.
21. Houchen, C. W., George, R. J., Sturmoski, M. A., and Cohn, S. M. FGF-2 enhances intestinal stem cell survival and its expression is induced after radiation injury. *Am. J. Physiol.*, *276*: G249–G258, 1999.
22. Okunieff, P., Wu, T., Huang, K., and Ding, I. Differential radioprotection of three mouse strains by basic or acidic fibroblast growth factor. *Br. J. Cancer Suppl.*, *27*: S105–108, 1996.
23. Garcia-Barros, M., Paris, F., Cordon-Cardo, F., Lyden, D., Rafii, S., Haimovitz-Friedman, A., Fuks, Z., and Kolesnick, R. Tumor response to radiotherapy regulated by endothelial cell apoptosis. *Science (Wash. DC)*, *300*: 1155–1159, 2003.
24. Harris, A. L. Hypoxia—a key regulatory factor in tumour growth. *Nat Rev Cancer*, *2*: 38–47, 2002.